Anal. Chem. **2007,** *79,* 4022−4030

Parallel Nanoliter Microfluidic Analysis System

Per Andersson,* Gerald Jesson, Gunnar Kylberg, Gunnar Ekstrand, and Gunnar Thorsén

Gyros AB, Uppsala Science Park, SE-751 83 Uppsala, Sweden

A parallel nanoliter microfluidic analysis system based on capillary action, centrifugal force, and hydrophobic barriers is described. The precision of 112 parallel volume definition operations is determined to 0.75% CV at 200 nL using the individual sample introduction structure. For 20 nL, the actual measurement error is the dominating factor, with a combined error of 1.9% CV. Individual dispensing as well as dispensing through a common distribution channel is described. The volume definition precision for the common distribution channel is 1.6% CV for 200 nL. Unlike the dominating forces in microliter-sized channel systems, we describe hysteresis effects as exerting a major influence, which needs to be considered in order to control the operation and design of discrete nanoliter fluidics. Hydrophobic patches at the corners of the rectangular channel control corner-enhanced wicking. Excellent flow control of 1 and 2 nL/s is achieved using a predefined spin program.

In comparison with conventional analysis systems, μ-TAS (micro total analysis system) have the potential to achieve faster analysis times, improve automation, consume less reagents, gain more information from less sample, and significantly increase throughput by running parallel analyses.[1]

The development of μ-TAS-based parallel analysis systems has shown to be demanding. In 2001, Cheng et al. showed six parallel analyses[2] using electroosmotic (EO) flow; however, despite more than a decade of research on electroosmotic (EO) pumping, parallel separation systems have been challenging to develop. Some of the challenges using EO-pumping-based systems have been described earlier.[3,4] With suppressed EO flow, conventional multicapillary DNA electrophoresis was transferred to a chip performing parallel separations on 384 samples.[5] At present, most of the μ-TAS systems use a continuously pumped approach, i.e., liquid is pumped from an inlet reservoir to an outlet reservoir, and in most cases the volumes of sample and reagents needed to interface with the chip are several orders of magnitude higher than the volumes used in the analysis. This is also true of the parallel multilayer elastomeric system proposed by Unger et al.,[4] where an additional issue of sample and reagent compatibility with the elastomeric material has to be resolved. Moreover, using a continuous flow system requires reliable liquid connections to the chip; a chip with 100 or more channels requires at least 200 electrodes for the simplest EO case,[6] or hundreds of low dead volume pressure connections for pressure-driven systems. It is difficult to eliminate error in such a system, particularly if a disposable chip format is used. Centrifugal analyzers enable the development of parallel analysis systems without external connections. Miniaturized centrifugal analyzers for microliter volumes were reported in 1973; these used a plastic disc with the same diameter (12 cm) as used in today's compact discs (CD).[7] In another microliter-range centrifugal system, a microfabricated burst valve was introduced to control a centrifugal enzymatic assay with a total analysis volume of 12 μL.[8] More recently, several groups have worked with similar microliter centrifugal analyzers.[1,9−12] Although microfabricated, this system is developed for conventional volume analysis, and if the definition of a μ-TAS system is the ability to manipulate and analyze unconventional submicroliter volumes, the centrifugal analysis system would require the handling of nanoliter-sized liquid plugs similar to those described earlier for pressure-driven systems.[13−17] In contrast to large-volume approaches, discrete nanoliter volumes are more significantly affected by surface forces relative to gravitational force. Consequently, there are significant differences when developing a total analysis system capable of handling discrete 20−200 nL volumes as compared to microliter-sized systems. At the micrometer channel size appropriate for nanoliter volumes,

* To whom correspondence should be addressed. Phone: +46-(0)18-566300. E-mail: per.andersson@gyros.com.

(1) Zoval, J. V.; Madou, M. J. *Proc. IEEE* **2004**, *92*, 140−153.
(2) Cheng, S. B.; Skinner, C. D.; Taylor, J.; Attiya, S.; Lee, W. E.; Picell, G.; Harrison, D. J. *Anal. Chem.* **2001**, *73*, 1472.
(3) Mitchell, P. *Nat. Biotechnol.* **2001**, *19*, 717−21.
(4) Unger, M. A.; Chou, H.-P.; Thorsen, T.; Scherer, A.; Quake, S. R. *Science* **2000**, *288*, 113−116.
(5) Emrich, C. A.; Tian, H.; Medintz, I. L.; Mathies, R. A. *Anal. Chem.* **2002**, *74*, 5076−5083.
(6) Harrison, D. J.; Fluri, K.; Seiler, K.; Fan, Z. H.; Effenhauser, C. S.; Manz, A. *Science* **1993**, *261*, 895−897.
(7) Scott, C. S.; Burtis, C. A. *Anal. Chem.* **1973**, *45*, 327A−340A.
(8) Duffy, D. C.; Gillis, H. L.; Lin, J.; Sheppard, N. F.; Kellogg, G. J. *Anal. Chem.* **1999**, *71*, 4669−4678.
(9) Madou, M. J.; Lua, Y.; Laib, S.; Kohb, C. G.; Leeb, L. J.; Wennerc, B. R. *Sens. Actuators, A* **2001**, *91*, 301−306.
(10) Steigert, J.; Grumann, M.; Brenner, T.; Riegger, L.; Harter, J.; Zengerle, R.; Ducrée, J. *Lab Chip* **2006**, *6*, 1040−1044.
(11) Haeberle, S.; Brenner, T.; Zengerle, R.; Ducrée, J. *Lab Chip* **2006**, *6*, 776−781.
(12) Madou, M.; Zoval, J.; Jia, G.; Kido, H.; Kim, J.; Kim, N. *Annu. Rev. Biomed. Eng.* **2006**, *8*, 601−628.
(13) Fujii, T.; Hosokawa, K.; Shoji, S.; Yotsumoto, A.; Nojima, T.; Endo, I. In *Micro Total Analysis Systems 98*; Harrison, D. J., van den Berg, A., Eds.; Kluwer Academic Publishers: Dordrecht, The Netherlands, 1998.
(14) Burns, M. A.; Johnson, B. N.; Brahmasandra, S. N.; Handique, K.; Webster, J. R.; Krishnan, M.; Sammarco, T. S.; Man, P. N.; Jones, D.; Heldsinger, D.; Mastrangelo, C. H.; Burke, D. T. *Science* **1998**, *282* (5388), 484−487.
(15) Hosokawa, K.; Fujii, T.; Endo, I. *Anal. Chem.* **1999**, *71*, 4781−4785.
(16) Handique, K.; Burke, D. T.; Mastrangelo, C. H.; Burns, M. A. *Anal. Chem.* **2000**, *72*, 4100−4109.
(17) Handique, K.; Burke, D. T.; Mastrangelo, C. H.; Burns, M. A. *Anal. Chem.* **2001**, *73*, 1831−1838.

10.1021/ac061692y CCC: $37.00
Published on Web 05/02/2007

capillary action dominates, either promoting or inhibiting the introduction of liquids into the micometer channels on the disk.

In this work we demonstrate a centrifugal analysis system able to work in the nanoliter range. First, capillary action is used for the imbibition (influx of liquid) of real samples, such as plasma or serum, into the 20 or 200 nL volume-defining chambers. To avoid filling the entire channel system, a hydrophobic barrier is used to stop liquid imbibition. Centrifugal force is then used to pressure liquid through the hydrophobic barrier; this enables the creation of a multiple parallel barrier system without needing connections to a chip. This microfluidic analysis system reproducibly and reliably performs more than 100 analyses in parallel. The system has been reported earlier running cell-based assays,[18] sample preparation for MALDI-MS,[19] and for protein quantification.[20,21] In this work we demonstrate a way of handling the fundamental parameters so as to achieve good analytical performance. The functionality and theory of the hydrophobic barrier, capillary action, corner-enhanced wicking, and flow rate is demonstrated. This results in a microfluidic design of the volume-defining function, both for individual and for commonly distributed samples and reagents, enabling the development of analytical systems for parallel nanoliter handling.

EXPERIMENTAL SECTION

Fabrication of Microstructures. The manufacturing of a replicated microfluidic CD has been described previously.[22] In this work the silicon CD master is etched with a multilevel, deep reactive, ion−etch process. A seed layer of conducting metal is sputter-deposited on the silicon wafer before electroforming. An electroplated nickel shim is then used as a mold insert to manufacture the CDs, by injection molding on a modified CD molding machine (Toolex Alpha AB, Sundbyberg, Sweden). The replicated CDs are molded in polycarbonate of bisphenol A (PC), Makrolon DP1-1265 from Bayer (Leverkusen, Germany) or Zeonor (Zeon, Japan). The discs are immersed in ethanol prior to oxygen plasma treatment (Plasma Science PS0500 reactor, AST, Billerica, MA). Details of this process together with further surface modifications are described elsewhere.[23,24]

The hydrophobic barrier is made by aligning a plastic or metal shadow mask over a CD and spraying a solution of fluorinated polymer over the shadow mask. A barrier is also made on the lid; this consists of a commercially available plastic lamination material with drilled holes 0.85 mm in diameter (DuPont, U.S.A.). A heat lamination procedure is used to bond the aligned lid to the CD. The contact angles of CD and lid are measured using an optical contact angle meter CAM 200 (KSV Instruments Ltd., Helsinki, Finland). Depth measurements are made using a Mitutoyo Quick Vision Elf Pro (Mitutoyo, Japan).

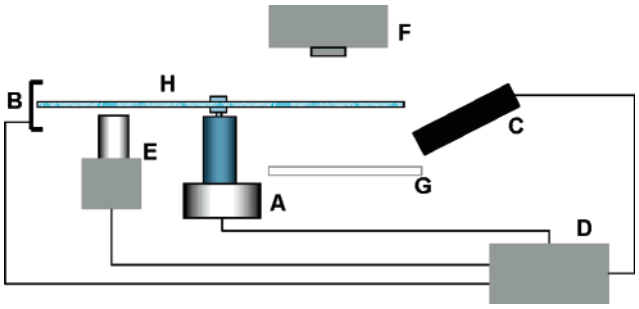

Figure 1. Schematic of the research prototype instrument: A = brushless dc motor; B = optical position sensor; C = stroboscope; D = controller; E = optical detector; F = video camera; G = white-light diffuser; H = CD device.

Spinner Setup. The CD spinner, see Figure 1, used to generate controlled centrifugal forces consists of a hub connected to a brushless dc motor with an integrated encoder (Minimotor 2444S 024 B, Minimotor SA, Croglio, Switzerland) and its control unit (Minimotor MCBL-50V-4A, Minimotor SA, Croglio, Switzerland), connected to a PC through an I/O control card (LAB PC 1200, National Instruments, Austin, TX). The rotational speed and position of the CD is controlled by in-house Labview software (National Instruments, Austin, TX). Programs controlling rotational speed from 0 to 10 000 rpm and acceleration from 0 to 6000 rpm/s, rotation of the disc to specific positions, and the control of the stroboscope enable the development of spin sequences. For safety, a protective hood and eye protection are used when spinning the CD.

A digital video microscope (DVM Kappa, Gleichen, Germany) is used to monitor and study the movement of liquids in the channels of the microstructure. The camera is connected to a digital video recorder (SONY GV-D900 E PAL, Sony, Tokyo, Japan), to enable video recording prior to analysis. The liquid flow is monitored during spinning by a stroboscope (Hella Optilux, Hella KG Hueck&Co, Lippstadt, Germany, or MVS 7060, PE optoelectronics, Salem, MA), which is triggered at each revolution by an indicator, either replicated on the CD or applied to the CD with adhesive. An optic sensor (OMRON E3X-F51, Tokyo, Japan) for the indicator is mounted on the setup. When the indicator on the disc passes the sensor a delay time is added; this is controlled by the software enabling the stroboscope to be triggered and a desired CD position to be viewed. All positions on the CD can be monitored while spinning the disc by controlling the delay time.

The hydrophobic barriers break-through pressure is determined by measuring the rpm at break-through (the critical rotational speed (CRS)). This is done using the CCD camera, operated at 25 frames per second (fps). The rotational acceleration is set to 200 rpm/s to register variations in CRS of the identical structures on the CD. The rpm resolution for this experiment is 8 rpm of acceleration per frame.

Imbibition Study. The CCD camera is used to document the time of imbibition from 5 to 20 mm into a 40 μm deep and 100 μm wide channel. The channels are dry, and a droplet of 3 μL of purified water is added to the channel at the end of the lid. Lid

(18) Thomas, N.; Ocklind, A.; Blikstad, I.; Griffiths, M.; Kenrick, K.; Derand, H.; Ekstrand, G.; Ellström, C.; Larsson, A.; Andersson, P. In *Micro Total Analysis Systems 2000*; van den Berg, A., Bergveld, P., Eds.; Kluwer Academic Publishers: Dordrecht, The Netherlands, 2000; pp 249−252.
(19) Palm, A.; Wallenborg, S. R.; Gustafsson, M.; Hedström, A.; Togan-Tekin, E.; Andersson, P. In *Micro Total Analysis Systems 2001*; Ramsey, M., van den Berg, A., Eds.; Kluwer Academic Publishers: Dordrecht, The Netherlands, 2001; pp 216−218.
(20) Rivera, E.; Ekholm Pettersson, F.; Inganas, M.; Paulie, S.; Gronvik, K. *Vaccine* **2005**, *23*, 5411−5419.
(21) Honda, N.; Lindberg, U.; Andersson, P.; Hoffmann, S.; Takei, H. *Clin. Chem.* **2005**, *51*, 1955−1961.
(22) Larsson, O.; Ohman, O.; Billman, A.; Lundbladh, L.; Lindell, C.; Palmskog, G. In *1997 International Conference on Solid State Sensors and Actuators*, Chicago, June 16−19, 1997; IEEE Catalog 6/1997; pp 1415−1418.
(23) Larsson, A.; Derand, H. *J. Colloid Interface Sci.* **2002**, *246*, 214−221.
(24) Johansson, B.-L.; Larsson, A.; Ocklind, A.; Öhrlund, Å. *J. Appl. Polym. Sci.* **2002**, *86*, 2618−2625. Image J, National Institutes of Health: http://rsb.info.nih.gov/ij/index.html (accessed Sep 2006).

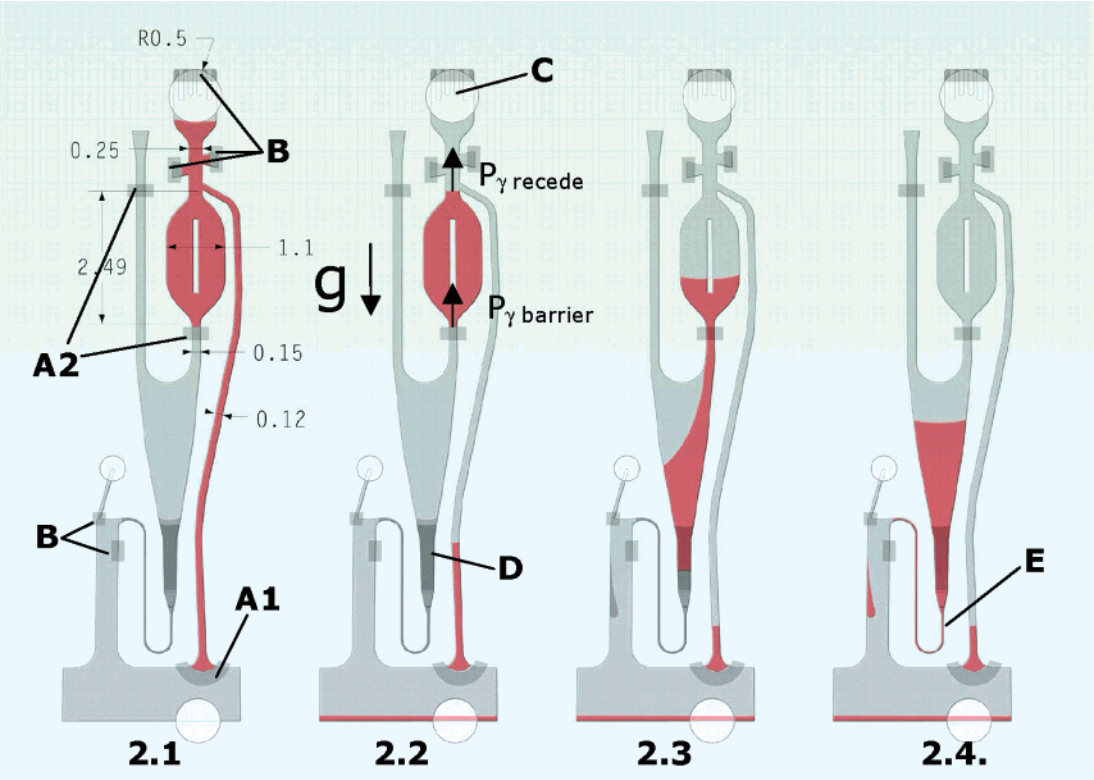

Figure 2. Close-up of analysis structure functionality. Symbols: A = hydrophobic barrier; B = hydrophobic patch; C = capillary posts; D = packed column; E = position of the channel cut off by the hot soldering iron, for volume measurement experiments. Part 2.1 shows liquid drawn in by capillary action. Part 2.2 shows the overflow channel activated at 1000 rpm removing excess liquid. Part 2.3 shows the volume (200 nL) defined within the chamber; a short pulse of a higher speed forces the liquid through the barrier. In part 2.4. a defined volume moves through the packed column at a constant flow rate by a spin speed program.

holes are not used as they can generate extra pressure from the droplet that can form at the hole.

Volume Definition. The precision of the volume definition in Gyrolab Bioaffy CDs, 20 and 200 nL sample volumes (Gyros AB, Uppsala, Sweden), is determined in the individual volume definition structures. The liquid is transferred to the CD and processed using a Gyrolab Workstation LIF (Gyros AB, Uppsala, Sweden). The channel is closed at the restriction channel (see Figure 2.4, E) by melting the channel shut with a hot soldering iron. A detection setup using a back-lit CD and the DVM video microscope is used to monitor the liquid level in the CD chamber, for subsequent import to Image J software.[25] These measurements are used for assessing liquid area and liquid area changes, which correspond to liquid volume and liquid flow rate. Due to difficulties associated with measuring the absolute volume, the 20 and 200 nL is calculated from the designed dimensions of the volume-defining unit in the plastic device. However, as most analytical techniques use relative measurements, the defined volume must be reproducible both inter- and intra-CD.

The volume-defining spin program is as follows:

rotation speed [rpm]	acceleration [rpm/s]	time [s]
0−1000	5000	0.2
1000	0	1
1000−3500	10000	0.25
3500−1000	−8333	0.3
1000−0	−5000	0.2

THEORY

Imbibition Model. Imbibition is the process whereby surface tension forces cause a liquid to flow into a micrometer channel. The curvature radius of the cylindrical surface of a liquid between two parallel vertical plates in a basin is directly given by

$$r_1 = d/(\cos(\theta_1) + \cos(\theta_2)) \quad (1)$$

where d is the distance [m] between the plates, θ_1 is the wetting angle at one plate, and θ_2 is the wetting angle at the other plate. The corresponding capillary pressure is given by the Laplace−Young equation:

$$p_{\gamma 1} = \gamma(\cos(\theta_1) + \cos(\theta_2))/d \quad (2)$$

where γ is the surface tension [N/m].

For a rectangular channel the pressure can be approximated by the combination of two perpendicular curvatures. The corresponding capillary pressure is

$$p_{\gamma \mathrm{rect}} = \gamma(\cos(\theta_1) + \cos(\theta_2))/a + \gamma(\cos(\theta_3) + \cos(\theta_4))/b \quad (3)$$

where a is the depth of the channel and b is the width. θ_1 is the wetting angle to the lid and θ_2 is the wetting angle to the bottom

(25) http://rsb.info.nih.gov/ij/index.htm.

of the channel. θ_3 and θ_4 are the wetting angles of the sides of the channel and are often equal to θ_2.

A spherical drop, radius r [m], applied to a channel inlet will generate a pressure, $p_{\gamma\text{in}}$, according to Laplace:

$$p_{\gamma\text{in}} = 2\gamma/r \tag{4}$$

Viscosity can be expected to be the main pressure opposing imbibition. The theoretical speed of imbibition is then controlled by the difference between the forces of viscosity and net imbibition.

The pressure drop [Pa] due to viscosity is given by a Newtonian fluid in a circular tube:

$$\Delta p_\mu = 32\mu v L/{D_\text{h}}^2 \tag{5}$$

where μ = viscosity of the liquid [Ns/m^2], v = mean flow speed [m/s] in the channel, and L = length [m] of the channel. If square channels are used, the hydraulic diameter [m] is $D_\text{h} \approx 4ab/(2a + 2b)$.

Since the net force causing imbibition is given by

$$\Delta p_\text{imb} = -p_{\gamma\text{rect}} + p_{\gamma\text{in}} \tag{6}$$

the rate of imbibition is determined by

$$\Delta p_\text{imb} = \Delta p_\mu \tag{7}$$

Thus, the velocity of imbibition is

$$v = (-p_{\gamma\text{rect}} + p_{\gamma\text{in}}){D_\text{h}}^2/(32\mu L) \qquad \text{[m/s]} \tag{8}$$

Hydrophobic Barrier Valve. The liquid is transported into the CD channels by imbibition and stopped by hydrophobic barriers, as the capillary pressure from the barrier is higher than that of the meniscus from the inlet end of the channel. For further processing the liquid is forced past the barrier by increasing the rotational speed until the centrifugal pressure overcomes the difference between the capillary pressures of the barrier and the back-end meniscus. The centrifugal driving pressure is given by the expression

$$\Delta p_\omega \equiv \Delta r r_\text{m} \omega^2 \rho \tag{9}$$

where Δp_ω is the centrifugal pressure difference [Pa], Δr is the radial height difference [m] between the barrier meniscus and the receding meniscus, r_m is the mean radius [m] between the barrier meniscus and the receding meniscus, ω is the angular speed of the CD [rad/s], and ρ is the density of the liquid [kg/m^3].

Considering contact angle hysteresis, the pressure from the hydrophobic barrier is given by

$$p_{\gamma\text{barrier}} = -\gamma(\cos(\theta_{a1}) + \cos(\theta_{ab}))/a_\text{barrier} - \gamma(\cos(\theta_{ab}) + \cos(\theta_{ab}))/b_\text{barrier} \qquad \text{[N/m]} \tag{10}$$

where γ is surface tension, θ_{a1} is the advancing angle of the liquid on the lid, θ_{ab} is the advancing angle of the liquid on the barrier, a_barrier is the depth of the barrier, and b_barrier is the width of the barrier. Viscosity is not considered here as the liquid plug is not moving.

Pressure from the back-end meniscus is given by

$$p_{\gamma\text{recede}} = -\gamma(\cos(\theta_{r1}) + \cos(\theta_{rc}))/a_\text{recede} - \gamma(\cos(\theta_{rc}) + \cos(\theta_{rc}))/b_\text{recede} \tag{11}$$

where θ_{r1} is the receding angle of the liquid on the lid, θ_{rc} is the receding angle of the liquid in the channel, a_recede is the depth [m] of the back-end meniscus, and b_recede is the width [m] of the back-end meniscus.

The required driving pressure for the liquid to start passing the barrier is given by

$$\Delta p_\gamma = p_{\gamma\text{barrier}} - p_{\gamma\text{recede}} \tag{12}$$

The pressure that must be exceeded to get the liquid through the barrier is given by

$$\Delta p_\omega \equiv \Delta p_\gamma \tag{13}$$

The corresponding rotational frequency is given by

$$f = \frac{1}{2\pi}\sqrt{\frac{p_{\gamma\text{barrier}} - p_{\gamma\text{recede}}}{\Delta r r_\text{m} \rho}} \qquad \text{[Hz]} \tag{14}$$

RESULTS AND DISCUSSION

The Gyrolab Bioaffy CD structure in Figure 3 shows a unit of eight parallel structures, all connected by a common distribution channel. Conceptually, the structure design is a chromatography system; loading, injecting, and column separation are all similar to a conventional chromatography system. Gradient elution is possible if a mobile phase is added on the fly[26] or by stepwise elution. Individual inlets and common distribution inlets, shown in Figure 3, deliver 200 nL to the column chamber. A spin program generating a constant flow over the column is used for enrichment, binding assays, reagent delivery, and wash steps. A postcolumn restriction channel determines the flow resistance to avoid flow differences induced by the pressure drop over the column. Unlike conventional systems, detection is performed on-column using a scanning confocal laser-induced fluorescent detector inside the Gyrolab workstation.

Filling by Capillarity. To fill the loading channel, capillary action at the inlet channels of the CD must be reliable. In previous CD analysis systems where 5−50 μL is used, liquid can enter the chambers without the use of capillary action. Filling of microliter-sized inlet channels is reported on unmodified plastics.[7−9,27,28] Owing to the small channel dimensions appropriate for the 20−

(26) Jesson, G.; Kylberg, G.; Andersson, P. In *Micro Total Analysis Systems 2003*; Northrup, M. A., Jensen, K. F., Harrison, D. J., Eds.; Transducers Research Foundation, Inc.: Cleveland, OH, 2003; pp 155−158.
(27) Johnson, R. D.; Badr, I. H. A.; Barrett, G.; Lai, S.; Lu, Y.; Madou, M. J.; Bachas, L. G. *Anal. Chem.* **2001**, *73*, 3940−3946.
(28) Badr, I. H. A.; Johnson, R. D.; Madou, M. J.; Bachas, L. G. *Anal. Chem.* **2002**, *74*, 5569−5575.

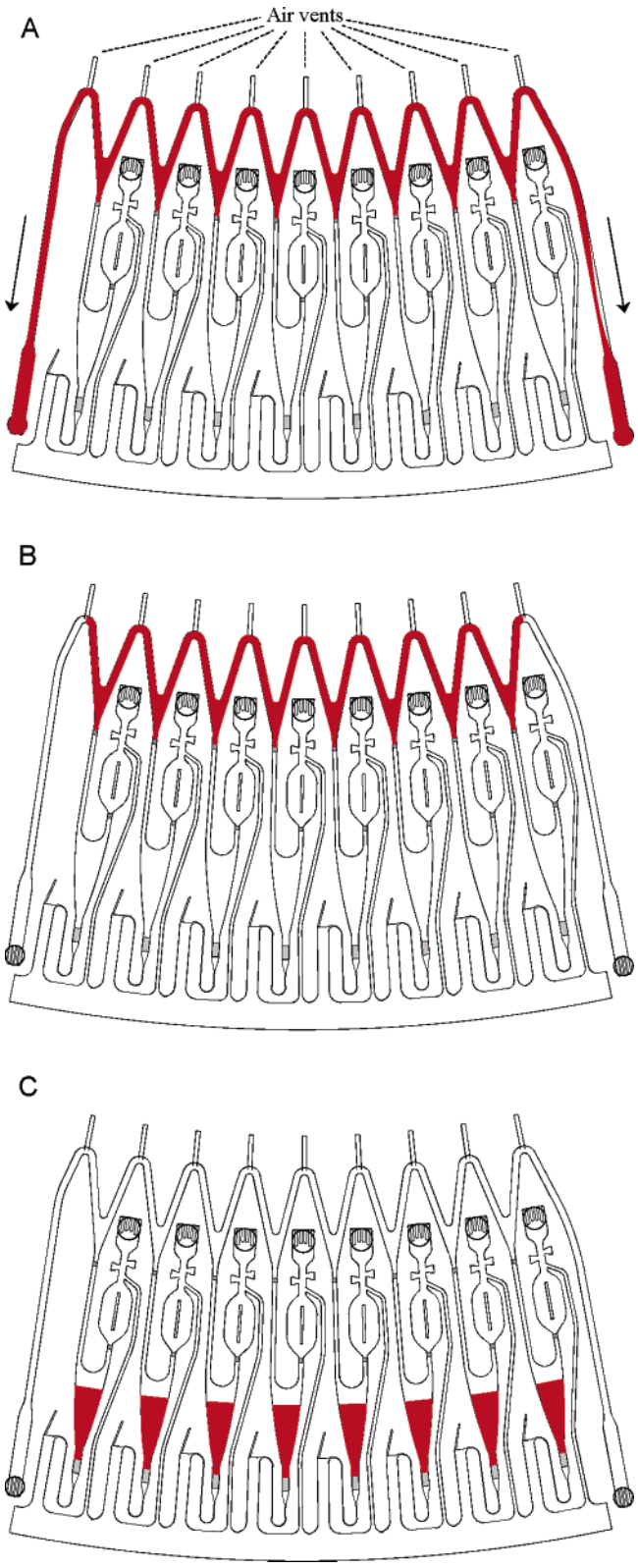

Figure 3. Gyrolab Bioaffy CD structure schematically drawn with a unit of eight parallel structures for analysis, all connected by a common distribution channel. (A) Common channel filled with a liquid. (B) At 1000 rpm the two side channels are released, thus volume defining the ends of structures 1 and 8. (C) At increased rpm, the air vents will split the liquid while it is moving down to the column chamber, thus generating eight discrete 200 nL plugs.

200 nL used in this work, reliable imbibition is not achieved using unmodified plastic materials.

To study the imbibing process, three molded bases with different surface treatments and three lids with different contact angles are combined. The surface treatment is generated using oxygen plasma treatment as described earlier.[23,24] Table 1 shows how the theoretical imbibition rate corresponds to the measured imbibition. Advancing contact angles are determined for both CD and lid materials to predict the imbibing flow rate. At higher contact angles the deviation between the model and measurement are in the order of 20-fold, and many of the channels fill only partially or not at all. In CDs with the most hydrophilic surfaces, deviations between the ratios for measured and modeled flow rates are a factor of 3 and channels fill reliably. As expected, the imbibition rate decreases with a higher advancing angle of the lid. In the most hydrophilic channels, the advancing angle of the lid has little effect on the imbibition rate. These significant experimental divergences from the theoretical flow rate are likely explained by the pinning forces that the contact line between the vapor−liquid−solid phases can encounter.[29,30] We observe reliable imbibition only when the advancing contact angle is less than 30° on the CD. As most of the common plastic materials used in injection molding have advancing contact angles higher than 30°, the surface of the CD is made hydrophilic by oxygen plasma treatment.

Hydrophobic Barrier. To stop the imbibing liquid filling the whole device, capillary barriers are used. One early approach for large-dimension channels and unmodified plastics was to use an abrupt change in channel cross section.[8,14] This approach was tested in-house without success using a hydrophilic channel system for discrete nanoliter handling. To create capillary barriers that work reliably in a hydrophilic device we developed a hydrophobic barrier approach described earlier.[31] In addition, the use of this approach allows repositioning of the barrier without needing to manufacture a new disc master. Handique et al.[16] developed a volume-defining system that used a hydrophobic patch, where the actuating principle was based on connecting gas pressure to the channel system to drive the liquids.

Critical Rotational Speed. In our work the properties of a simple hydrophobic barrier are investigated and modeled using centrifugal force as the actuating principle. For each barrier acting as a valve, there is a CRS at which centrifugal force generates enough pressure on the liquid plug to overcome the threshold pressure of the hydrophobic barrier, thus forcing the liquid to pass through the channel. The pressure generated in the plug is described in eq 9. To create a predictive model for the valves actuation in our CD, we have developed a theoretical model for the threshold pressure. For microchannel surfaces that are not homogeneous, such as molded plastic surfaces, there will be areas on the disk that present barriers to the motion of the contact line. This will generate advancing and receding contact angles. The experimental versus theoretical rpm for overcoming the hydrophobic barrier is shown in Figure 4. The model considers the contact angle hysteresis, defined as the difference between the maximum (advancing) and minimum (receding) contact angle values. Hysteresis was earlier considered in a work describing

(29) Schäffer, E.; Wong, P.-Z. *Phys. Rev. Lett.* **1998**, *80*, 3069−3072.
(30) Wilson, D. J.; Pond, R. C.; Williams, R. L. *Interface Sci.* **2000**, *8*, 389−399.
(31) Andersson, P.; Almer, K.; Larsson, A. Microfluidic Device. International Patent Application WO9958245A1, 1999.

Table 1. Calculated and Measured Imbibition Rates Using Different Prepared CD and Lid Combinations

advancing contact angle CD	85°		44°		4°		
advancing contact angle lid	77°	86°	77°	86°	77°	86°	106°
theor flow rate [mm/s]	8.0	5.2	23.8	21.0	30.8	27.9	21.5
exptl flow rate [mm/s]	0.4 ± 0.5	0.3 ± 0.2	2.9 ± 0.5	2.6 ± 0.3	11.2 ± 0.4	7.4 ± 0.8	8.6 ± 0.7
ratio between theor and exptl flow rate	20.1	16.2	8.1	7.9	2.8	3.8	2.5

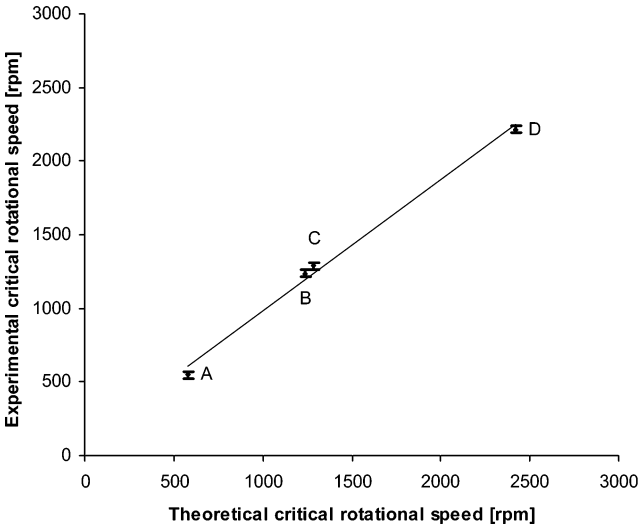

Figure 4. Experimental vs theoretical CRS for overcoming the hydrophobic barrier using water. The channel dimensions (depth × width) for the advancing and receding menisci are (A) advancing 100 × 850 μm^2, receding 100 × 1000 μm^2, (B) advancing 100 × 200 μm^2, receding 100 × 700 μm^2, (C) advancing 100 × 150 μm^2, receding 100 × 250 μm^2, and (D) advancing 40 × 40 μm^2, receding 100 × 100 μm^2.

thermopneumatic pumping on a chip.[32] In a later work the same group predicted that there could be a threshold pressure impact on their volume definition process due to contact angle hysteresis.[17] The theoretical model used here to predict the centrifugal force required to cause liquid to flow past a given hydrophobic barrier is shown in eq 12. The threshold pressure relies on the following: (1) the channel dimension at the barrier; (2) the dimensions of the back-end meniscus; (3) the surface tension; (4) the advancing angle for the liquid on the barrier; (5) the receding angle for the liquid in the channel and lid.

The effect of hysteresis according to eq 11 shows that the back-end channel dimensions and its receding contact angle have an effect on the CRS. Consequently, a different back-end meniscus will require a different CRS. Figure 5 shows how the CRS is influenced by changes in the relative sizes of the two menisci. Note the steep change in threshold pressure for ratio values below 1, i.e., where the receding meniscus is smaller than the barrier meniscus. This gives considerable design flexibility when choosing the threshold pressure. However, small changes in the dimensions of the actual fabricated channel at ratios under 0.5 may lead to significant differences in channel-to-channel CRS. There is a less-pronounced effect on the threshold pressure for ratios of more than 1 if the channel is fabricated with only one depth than when more depths are allowed. This shows that the back-end dimensions in a discrete nanoliter-sized microfluidic system must be considered in the design of microfluidic systems controlled by surface forces. Another interesting effect of hysteresis is that the valve is also functional at an advancing contact angle of 60°, curve A in Figure 5, which by definition is a hydrophilic barrier.

Reliability of the Hydrophobic Barriers. Reliability of the hydrophobic barriers is of utmost importance. Also, time-critical operations such as mixing rely on simultaneous valve actuation. To evaluate the reliability of valves, repeated volume definitions, described in Figure 2, are used to test deviation of CRS of the barriers used in the volume definition process. A total of 590 valve actuations, distributed over three different Gyrolab Bioaffy CDs, are recorded as described in the Experimental Section. The structures on each CD are reused at least twice. The minimum recorded CRS is 1612 rpm, and the maximum CRS is 1700 rpm, i.e., a span of 88 rpm. No large variation between the CDs is noted, inter-CD precision is 0.4% CV for the lowest recorded CRS and 0.7% CV for the highest recorded CRS. No systematic effects are recorded for the parallel valves within a CD or for a valve being actuated repeatedly. With such a narrow span between CRS_{min} and CRS_{max}, it is theoretically possible to have several consecutive valves coupled in series within one microfluidic analysis structure. Water, as used in the above experiment, is rarely used in life science applications. The hydrophobic valve relies on surface tension forces of the liquid used. In biological systems a wide range of compounds such as proteins, detergents, and organic modifiers are used. To ensure compatibility with commonly used reagents, we investigated the effect of a number of frequently used reagents. A Gyrolab Bioaffy CD can be used with water more than 40 times depending on surface treatment, type of hydrophobic polymer, and the types of solutions used. For 1% BSA solution the CD can be used at least three times without failure. It is also possible to reliably manipulate the following reagents using a CD at least once: 0.01% Tween, 70% ACN, 100% MeOH, and anticoagulated whole blood.

Corner-Enhanced Wicking. When using square-shaped hydrophilic channels as in the CD, a flow due to corner-enhanced wicking can be induced[33] and will vary according to the liquid. In our work we control this effect by introducing hydrophobic barriers at the corners of the cross section of the channels. Without hydrophobic barriers we observed discrete liquid plugs inside the CD that relocate from their original position within minutes both during spinning and at rest. The corner-enhanced

(32) Sammarco, T. S.; Burns, M. A. *AIChE J.* **1999**, *45*, 350−366.
(33) Dong, M.; Chatzis, I. *J. Colloid Interface Sci.* **1995**, *172*, 278−288.

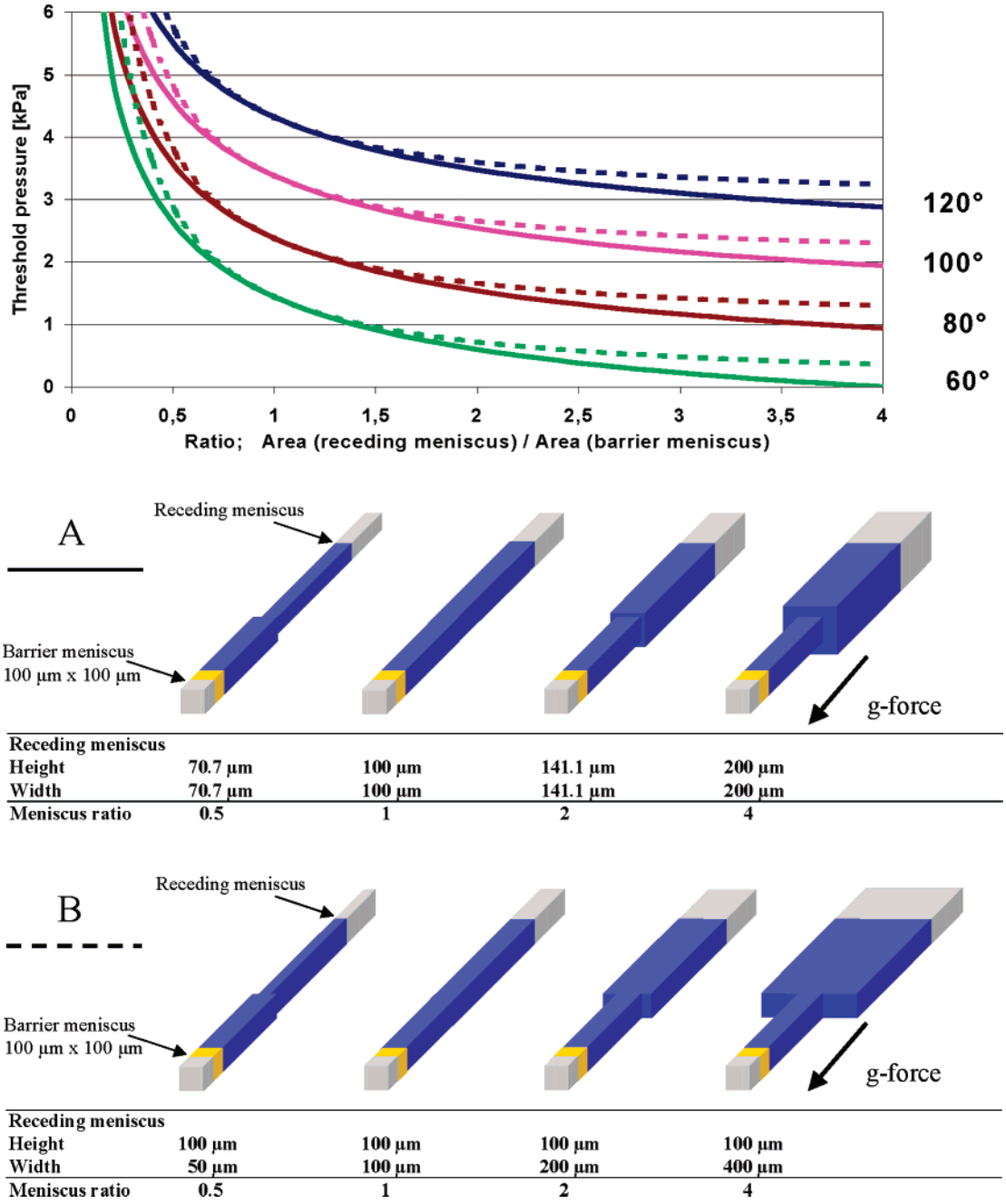

Receding meniscus				
Height	70.7 µm	100 µm	141.1 µm	200 µm
Width	70.7 µm	100 µm	141.1 µm	200 µm
Meniscus ratio	0.5	1	2	4

Receding meniscus				
Height	100 µm	100 µm	100 µm	100 µm
Width	50 µm	100 µm	200 µm	400 µm
Meniscus ratio	0.5	1	2	4

Figure 5. Receding meniscus influences threshold barrier pressure. In this model, the receding angle is set to 30° and the barrier meniscus is kept at a constant capillary dimension (100 × 100 μm^2). The theoretical threshold pressure is plotted against the barrier and receding (back-end) area ratios for different advancing angles. Solid lines represent the change in receding meniscus ratios where both depth and width are increased at a constant ratio (A). The dotted lines represent channel geometries where only the receding width is altered, as represented in part B.

wicking transport is only limited by the viscosity and can be observed by video microscopy using a colored liquid. Figure 6A show a finite element method (FEM LAB) simulated channel with corner-enhanced wicking. If evaporation can occur at an inlet or outlet hole, wicking will allow all liquid in a plug positioned millimeters away from the inlet hole to be transported to this evaporation zone. If a channel contains a liquid plug, liquid will flow along the corners, driven by a concave meniscus surface when the contact angle is below 45°. If the contact angle is greater than 45°, the surface would be convex and no corner-enhanced wicking would be induced. Figure 6B shows a FEM simulation of a CD channel where the two corners facing the lid show a less-pronounced flow (due to a different contact angle) than those corners not in contact with the lid. The hydrophobic barriers controlling the corner-enhanced wicking are illustrated as B in Figure 2.1, where the protruding structures are easy to coat with hydrophobic polymer. They serve as wicking barriers when the back-end meniscus has passed the protruding structures, either due to evaporation or to activated overflow. Possible enrichment effects at the volume definition meniscus are removed through the overflow channel as illustrated in Figure 2.2. We have measured wicking flow rates between 1 and 500 nL/min; this rate is dependent on factors such as contact angle, liquid properties, and evaporation area/conditions. Obviously, it is vital for the

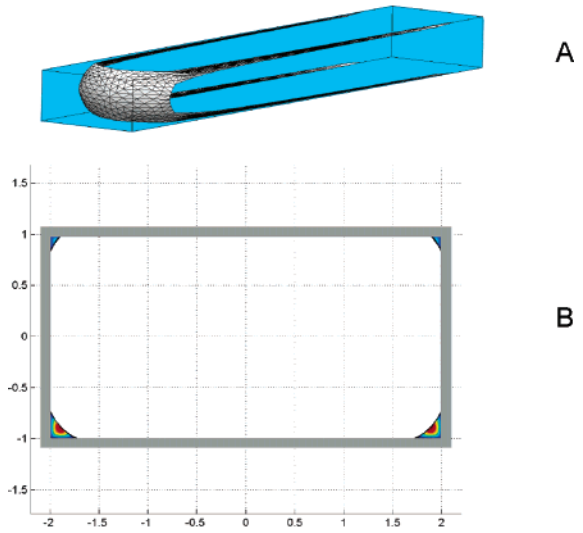

Figure 6. FEM simulation of the wicking process. (A) 3D projection of wicking into an empty channel. (B) Visualization of the magnitude of wicking in a rectangular 100 × 200 μm^2 channel. The red color indicates higher flow rates.

functionality of discrete microfluidics to control the corner-enhanced wicking phenomena.

Volume Definition Precision. Capillary action fills the volume definition channel, Figure 2.1, minimizing the total sample consumption to within the nanoliter range. The ridges at the inlet hole act as spacers, allowing liquid to pass out of transfer tips with minimal obstruction. A hydrophobic patch partially covering the inside of the inlet serves to direct the droplet toward the capillary inlet, minimizing the wetted area and thus reducing sample consumption. It is important to overfill the inlet port to achieve reliable volume definitions. To create an exact volume on the disk, the overflow channel is activated when barrier A1 in Figure 2.1 is opened by spinning the disk at 1000 rpm. After less than a second the volume is defined as in Figure 2.2. To transfer the volume to the packed bed, a short spin pulse to 3500 rpm is used to open the barrier, and the liquid transfers down into the column chamber, Figure 2.3.

The precision of a volume-defined discrete liquid was reported by Handique et al.[16] to depend on the size of the splitting junction in relation to the length of volume definition channel in their air pressure system, but no statistical data was presented. Another potential error is the reproducibility of the dimensions in the volume definition structure. Measurement of the dimensions of the volume definition channel show no significant variation. The channel in the replicated plastic CD has less than 1% CV (both intra-, $n = 112$, and inter-CD, $n = 3$) in depth for the measured channels.

We determine the relative error of volume definition in the structure shown in Figure 2 containing approximately 200 nL by assessing liquid area and liquid area changes. Five different CDs using 112 channels on each CD are run with water; the manual cutoff procedures (melting the channel shut) fail in 9 of the channels and are excluded from the 551 data points represented in Table 2. A precision of 0.75% CV shows the precise volume definition achievable on this system. The precision using water in the common distribution channel, 8 × 200 nL shown in Figure 3, is determined to a CV of 1.6%. Error resulting from differences

Table 2. CV from Volume Definition Experiment[a]

	CD1	CD2	CD3	CD4	CD5	all data points
average	4884	4867	4891	4877	4880	4880
SD	40	41	39	33	26	37
CV (%)	0.81	0.83	0.79	0.67	0.53	0.75

[a] A total of 112 volume definitions of human plasma were measured on 5 different CDs using a video camera and Image J. The measurement error was determined to 0.25% CV.

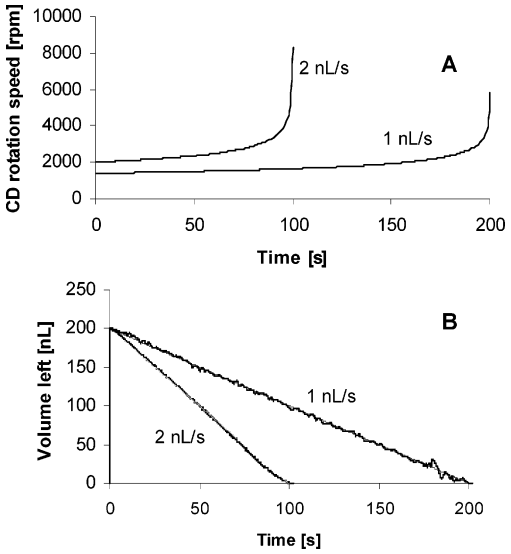

Figure 7. (A) Generated spin program derived from experiments and fitted into eq 9 to generate 1 and 2 nL/s flow rates of human plasma through the Gyrolab Bioaffy CD. (B) The resulting flow rates in black are measured and compared with the theoretical flow rate in gray.

in position of the manual blocking of structures is calculated to 0.23% CV, resulting in that the CV can be misleadingly high. For the 20 nL inlet structure a CD is evaluated using human plasma where four cutoff procedures failed, leaving 108 data points giving a CV of 1.9%. The error resulting from differences in position of the manual blocking of structures is now calculated to 2.3% CV and should be the dominating factor. The 20 nL volume definition structures are identical to the 200 nL but for the volume chamber which is 100 × 100 × 2000 μm^3 in depth/width/length.

Constant Flow Rate. Constant flow rate is important in many analytical applications. The absolute flow rate depends on flow resistance over the particle bed and outlet channels, viscosity of the liquid, and advancing and back-end meniscus contribution, as described in the Theory section. The resistance of the CD channel flow path is empirically determined using different starting pressures. For example, the flow rate versus time is monitored at constant 1000 rpm and the experiment is repeated for 2000 and 3000 rpm. The resulting declining flow rate profiles (curve equations), in combination with the geometry of the column chamber are then fitted into eq 9 to generate a spin program for controlled nanoliter/second flows in the CD. For the Gyrolab Bioaffy CD[20,21] the spin program of 1 and 2 nL/s for human plasma through a particle bed of 15 μm beads is shown in Figure 7A. The results obtained by measuring the flow rate using video capture show good correlation with the calculated flow rate, Figure 7B.

CONCLUSION

Our understanding of the effect of parameters such as contact angle hysteresis, liquid pinning, and multiple menisci, as outlined in this paper, has allowed the development of a parallel, discrete nanoliter microfluidic analysis system. We have considered the scaling effects for discrete nanoliter liquid volumes and combined a range of functionalities that enable construction of an automated parallel analysis system.

Handling liquid volumes in the nanoliter range requires evaporation control, a surface that minimize unwanted adsorption, corner-enhanced wicking control, flow control, and a reliable valve control to form a functional analysis system. No external connections to a chip are needed to drive flow when centrifugation is used to create the propulsion force. This enables parallel analysis at these low reaction volumes. The precision of microfabrication allows for precise analysis in the nanoliter range which is not possible when using conventional fabrication methods. The excellent precision for inter- and intra-CD volume definition supports the high-precision analytical results we have shown earlier in application-related work. The functionalities shown in this work enable reliable, automated, high-precision liquid handling of demanding samples such as serum in the submicroliter range that is not possible using current conventional technologies. In addition, the simple instrumentation needed for centrifugation analyzers will significantly reduce the need for complex software development and decrease failure associated with the number of mechanical devices needed in a conventional automated system.

ACKNOWLEDGMENT

We thank Stephan Hoffmann and Richard Cassidy for help with the manuscript and Fredrik Andersson for his contribution to the imbibition studies.

Received for review September 7, 2006. Accepted February 8, 2007.

AC061692Y